LIDAR ALGORITHMS FOR ATMOSPHERIC SLANT-RANGE VISIBILITY, PLANETARY BOUNDARY LAYER HEIGHT, METEOROLOGICAL PHENOMENA AND ATMOSPHERIC LAYERING MEASUREMENTS

Alexandros Pantazis[1*], Alexandros Papayannis[1], and Georgios Georgoussis[2]

[1]*National Technical University of Athens, Laser Remote Sensing Laboratory, Physics Department, 15780 Zografou, Greece, *Email: alexpant@mail.ntua.gr*

[2]*Raymetrics S.A., Spartis 32, 14452 Metamorfosi, Athens, Greece*

ABSTRACT

In this paper we present a method to estimate, in real time, the slant-range visibility, the Planetary Boundary Layer height (PLBH), the aerosol layers and other meteorological parameters, based on single or multi-wavelength lidar data. The lidar system can be operated at vertical (to calibrate the lidar system in a molecular atmosphere), 2-dimensional (2D) or 3-dimensional (3D) scanning mode. The algorithms developed are briefly, presented here along with several examples using real lidar data to estimate the PBLH, slant-range visibility and aerosol layering.

1. THE LADDER TECHNIQUE

There has been a lot of questioning on whether aerosol backscatter $\beta_{aer}(\lambda,R)$ and extinction $\alpha_{aer}(\lambda,R)$ coefficients can be derived from operational lidar slant range measurements without any large error estimations, resulting from assumptions like atmospheric homogeneity conditions presumed, in a large scale (e.g. typically over a few hundred meters) and on automatic retrieval of these values [1], [2]. The well-known lidar equation for the power received at wavelength λ from a distance R, is:

$$P(\lambda,R)=P_{OL}\cdot\frac{A_0}{R^2}\cdot\beta(\lambda,R)\cdot\eta(\lambda)\cdot\xi(R)\cdot\Delta R\cdot\exp^{-2\int_0^R[\alpha_{aer}(\lambda,r)+a_{Ray}(\lambda,r)]dr} \quad (1)$$

where, P_{0L} is the power of the transmitted laser pulse beam, A_0 is the diameter of the receiving telescope, $\beta(\lambda,R)$ is the atmospheric backscatter coefficient, ΔR is the spatial resolution of the lidar system, η(R) is the lidar opto-electronic efficiency coefficient, ξ(R) is the geometrical form (overlap) factor, and $a_{aer}(\lambda,r)$ and $a_{Ray}(\lambda,r)$ are the Mie and Rayleigh extinction coefficients of the atmospheric particles and molecules, accordingly.

Using Klett's technique [4, 5] this equation can be solved for $\alpha_{aer}(\lambda,R)$ and $\beta_{aer}(\lambda,R)$ in a way where:

$$a_{aer}(\lambda,R)=\frac{\exp[S(R)-S(R_F)]}{\frac{1}{a(\lambda,R_F)}+2\int_R^{R_F}\exp[S(R')-S(R_F)]dR'}-a_{Ray}(\lambda,R) \quad (2)$$

and

$$\beta_{aer}(\lambda,R)=\frac{\exp[S'(R)-S'(R_F)]}{\frac{1}{\beta(\lambda,R_F)}+2\int_R^{R_F}\frac{1}{C(R')}\exp[S'(R')-S'(R_F)]dR'}-\beta_{Ray}(\lambda,R) \quad (3)$$

where,

$$S'(R)-S'(R_F)=S(R)-S(R_F)-\frac{16\pi}{3}\int_R^{R_F}\beta_{Ray}\left(1-\frac{3}{8\pi\cdot C(R')}\right)dR' \quad (4)$$

and

$$S(R)\equiv\ln[P'(\lambda,R)\cdot R^2]=RCS \quad (5)$$

where, R_F is a reference height where the values of $\alpha(\lambda,R)$ and/or $\beta(\lambda,R)$ are known (e.g. for a purely molecular atmosphere), RCS is the Range squared-Corrected lidar Signal, after atmospheric and electronic BackGround (BG) noise subtraction, as:

$$P'(\lambda,R)=P(\lambda,R)-BG \quad (6)$$

and, C(λ,R) is the so-called lidar ratio:

$$C(\lambda,R)=a_{aer}(\lambda,R)/\beta_{aer}(\lambda,R) \quad (7)$$

It is obvious that in vertical pointing measurements, there is an aerosol-free height, where we can set the $\alpha(\lambda,R)$ and/or $\beta(\lambda,R)$ equal to their molecular values. So, the reference height R_F of Eq. (1) is the vertical height above which the atmosphere is purely molecular.

Scanning the atmospheric volume by a 3-dimensional (3D) scanning lidar, using the novel LADDER technique, we will show that we can retrieve $\alpha_{aer}(\lambda,R)$ and/or $\beta_{aer}(\lambda,R)$ by making measurements like "stair steps" from vertical to horizontal direction, every 1°, like "walking down a ladder" (cf. Fig. 1).

In this way, we take as R_F at Eqs. (2) and (3), the distance at which we abstract 1-2 slant - height bins (1 bin is equal to the spatial resolution ΔR) for every new measurement and we retain the last value of $\alpha_{aer}(\lambda,R)$ and/or or $\beta_{aer}(\lambda,R)$, at which R_F was previously taken, as the new calibrating values for $\alpha_{aer}(\lambda,R)$ and/or $\beta_{aer}(\lambda,R)$.

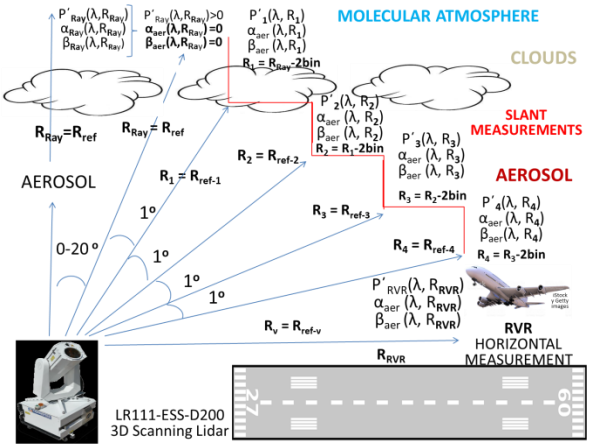

Fig. 1. The LADDER technique working principle (RVR-Runway Visual Range).

So, if R_F, $\alpha_{aer}(\lambda,R)$, $\beta_{aer}(\lambda,R)$ are the last known values and $R_{F\text{-}new}$, $\alpha_{aer}(\lambda,R_{new})$, $\beta_{aer}(\lambda,R_{new})$ are the new ones, then we have:

$$R_{F-new} < R_F \quad \textbf{(8)}$$

$$R_{F-new} = R_F - N_{bin} * \Delta R \quad (\text{where } N_{bin}=1, 2, 3, \text{etc.}) \quad \textbf{(9)}$$

In this way, from each sequential lidar measurement we can retrieve the corresponding $\alpha_{aer}(\lambda,R)$ and/or $\beta_{aer}(\lambda,R)$ values, taking into account the previous (last-known) values of these coefficients and by reducing R_F at the same time, there is a continuous "calibration" of these values, from the previous to the next "lower" position of R_i (i=1, 2, 3, etc.) (cf. Fig. 1).

And so, for every height "drop" we make towards to the horizontal position, we are able to evaluate the values of $\alpha_{aer}(\lambda,R)$ and/or $\beta_{aer}(\lambda,R)$ from the vertical position to the final (horizontal) one, thus avoiding the ambiguities related to assumptions, like presuming homogeneous atmospheres, which produces large errors, especially over long distances.

However, in the LADDER technique, we also assume a kind of atmospheric "homogeneity" based on the $a_{aer}(\lambda,R)$ or $\beta_{aer}(\lambda,R)$ values, between successive equidistant atmospheric layers (by moving by 1° in every step, each successive atmospheric layer has a depth of 100 m over a horizontal distance of about 5.9 km). The limit of 1° is user adjustable towards to more precise measurements, depending on the instability of the weather conditions. The more unstable or "heavy" the weather conditions are, the less the limit of 1° measurements can be reached.

Methods like the slope technique or the ratio method [3], are mainly using the assumption of homogeneous atmospheres over longer distances, to provide slant range atmospheric parameters; however in this way, the error on the derived parameters increases due to the instability of the prevailing atmospheric conditions, as a function of distance R. Other methods like the multiangle one [3], assume that a horizontal constant value of $\beta_{aer}(\lambda)$ is present at any distinct height, which is not the case for the LADDER technique and "real" atmospheres.

Moreover, the Optical Depth Solution according to [3] assumes that the aerosol backscatter to extinction coefficient is constant and the optical depth must be estimated by other independent measurements, in the vertical direction, like from a solar radiometer, or by a Raman lidar [6]. Even if this method seems to work well under different atmospheric conditions, the problem becomes noticeable when trying to make slant-horizontal range measurements, where this value cannot be retained as constant and cannot be found, especially in horizontal measurements and in longer ranges, where the lidar signal may become too noisy.

Furthermore, the LADDER technique maybe compared to the Boundary Point Solution (BPS) [3]. BPS assumes that the aerosol backscatter to extinction coefficient is constant and range-independent and sets the extinction coefficient as a known value at a specific range (boundary conditions). The same technique was used by Klett [4,5] (cf. Eqs. 2 and 3) and this setting of initial conditions is the only similarity with LADDER technique: in this technique, after the first vertical lidar measurements and the use of denoising algorithms, the reference (maximum) height is calculated, such as the values of $\alpha_{aer}(\lambda,R)$ and/or $\beta_{aer}(\lambda,R)$ become zero. Then, it is easier to retrieve $\alpha_{aer}(\lambda,R)$ and/or $\beta_{aer}(\lambda,R)$ for lower heights from the lidar signal.

So, with the LADDER technique and using the above mentioned equations (Eqs. 2 and 3), we expand this way of thinking, for slant and horizontal range measurements with different lidar ratio values, each time, taken from the METCON algorithm for each measurement of interest, dependent on the type of the desired detection (e.g. thin fog, moderate fog, haze, etc.).

Regarding the visibility slant range measurements, according to WMO and ICAO rules for daytime visibility and by using the empirical and well qualified, Koschmieder law (at 550 nm), the visibility Vis (in km) versus the atmospheric extinction α (in km^{-1}) is given by [2]:

$$Vis = 3/\alpha_{aer}(\lambda,R) \quad (\text{for } \varepsilon=0.05 \text{ at } 550 \text{ nm}) \quad \textbf{(10)}$$

$$Vis = 3.912/\alpha_{aer}(\lambda,R) \quad (\text{for } \varepsilon=0.02 \text{ at } 550 \text{ nm}) \quad \textbf{(11)}$$

where, ε is a pure number, showing a contrast threshold, as a difference of the self-luminance of any object and the general luminance of the area viewed from a standing position. The contrast threshold of 0.02 gives superior results to that of the value of 0.055 [1].

Therefore, the estimated error of the retrieved Vis values directly depends on the accuracy of the retrieved values of $\alpha_{aer}(\lambda,R)$ and/or $\beta_{aer}(\lambda,R)$. When the classic Klett's inversion method is implemented [4,5], where a constant $C(\lambda,R)$ value is used as input (constrained to the mean aerosol optical depth (AOD) obtained from a nearby sun photometer [7] the $\alpha_{aer}(\lambda,R)$ values are retrieved with an uncertainty of the order of 20–30% [8]. By using the

Raman technique (during nighttime) [6] retrieved the $\alpha_{aer}(\lambda,R)$ vertical profiles with uncertainties of ~5-15%.

The error estimation for the LADDER technique at the initial (vertical) lidar pointing measurement, concerning the product retrieval of the $\alpha_{aer}(\lambda,R)$ and/or $\beta_{aer}(\lambda,R)$ depends only on the error estimation of the method used (e.g. Klett or Raman). In our case of a non-homogeneous atmosphere and using the Klett method, we assume that we can obtain the values of $C(\lambda,R)$ (by taking the ratio of the values of $\alpha_{aer}(\lambda,R)/\beta_{aer}(\lambda,R)$) and the ranges of $a_{aer}(\lambda,R)$ for different types of aerosols (thin fog, haze, light haze, etc.). In this case we have overpassed the problem of the $C(\lambda,R)$ uncertainty for these types of atmospheric conditions [4,5], thus we obtain the profile of $\alpha_{aer}(\lambda,R)$ and/or $\beta_{aer}(\lambda,R)$ without any error related to the assumed value of $C(\lambda,R)$.

Then, if we are interested in the calculation of the visibility, we can derive its uncertainty (ΔVis) by taking the derivative of the visibility (Eqs. 10 or 11):

$$\Delta Vis = Vis * [\Delta\alpha_{aer}(\lambda,R)/\alpha_{aer}(\lambda,R)] \qquad \textbf{(12)}$$

where $\Delta\alpha_{aer}$ denotes the estimated error value of extinction coefficient.

Method	α_{aer} error ($\Delta\alpha_{aer}$) %	Vis error (ΔVis) %	Comments
Klett	20-30	20-30	Homogeneous atmosphere
Raman	5-15	5-15	Homogeneous atmosphere
LADDER	0 (as the value of $C(\lambda,R)$ is known)	0 (as the value of $C(\lambda,R)$ is known)	Homogeneous/ Non homogeneous atmosphere
Scatterometer	N/A	±10 m or ±10 %, highest values applies	Homogeneous atmosphere

Table 1. Various methods and techniques used to derive/estimate the atmospheric extinction and/or visibility and their associated uncertainty, compared to the LADDER technique in homogeneous/non homogeneous atmospheres.

In Table 1 we present the various methods and techniques used to derive/estimate the atmospheric extinction and/or visibility and their associated uncertainty, compared to the LADDER technique, in homogeneous/non homogeneous atmospheres. The error on the $\alpha_{aer}(\lambda,R)$ and/or $\beta_{aer}(\lambda,R)$ estimation (as well as on the Vis) is approximately zero, according to the explanation, previously provided.

It is worth noting that the LADDER technique is unique and can be applied in both homogeneous and non-homogeneous atmospheres, in contrast to the other techniques/methods which assume homogeneous atmospheric conditions over short/long distances. This advantage makes the LADDER technique more attractive in operational–commercial lidars and generally, in atmospheric visibility devices.

2. NAVIS-T/P ALGORITHM

After the use of denoising filters and the choice of the slant range measurement technique, the NAVIS (Novel Algorithm for VISibility measurement) – T (Tower of the Airport)/P (Pilot) algorithm can be applied for further lidar signal processing. This algorithm is able to determine the visibility of tower towards to the pilot and vice versa, according to WMO and ICAO rules of daytime visibility, at the airports.

Below, at METCON algorithm there are values of $\beta(\lambda, R)$ and $\alpha(\lambda, R)$ (Figs. 2, 3) as a function of wavelength λ, under different atmospheric conditions MAPP (Modular Atmospheric Propagation Program) as developed by SRI (Stanford Research Institute) [9]. Additionally, Measures [10] also provides another figure, where a number of different atmospheric conditions are taken into account (fog, haze, etc.) showing the atmospheric extinction coefficient versus visibility at 550 nm during daytime.

Then, we make use of the values of $\alpha_{aer}(\lambda,R)$ and/or $\beta_{aer}(\lambda,R)$ at the wavelength of interest, in combination with the atmospheric attenuation coefficient values to incorporate them into the NAVIS algorithm. Then, the AOD (Aerosol Optical Depth) (τ) (Eq. 13) can be calculated from the lidar – tower point of view towards the maximum range of the lidar signal and from the maximum range of lidar's signal, towards the lidar device near the runway (pilot's point of view):

$$\tau_{C_n}(0,R) = \int_0^R a_{C_n}(\lambda,R')dR' \qquad \textbf{(13)}$$

$$\tau_{total}(0,R) = \tau_{C_1} + \tau_{C_2} + \ldots + \tau_{C_n} \qquad \textbf{(14)}$$

where, R′ is the distance at which $\alpha_{aer}(\lambda,R)$ has been measured with a range resolution, typically, of 1-2 range bins, τ_{total} is the sum of τ_{Cn} and τ_{Cn} is the optical depth we use at the METCON algorithm (cf. section 3).

The visibility (towers' and pilots') is calculated and a categorization of atmospheric conditions–layering is been made at slant and/or vertical pointing lidar direction. So, with a 3D scanning lidar system, a profile of fully atmospheric layering at different angles, azimuth and vertical, can be provided in near-real time. In addition, the daytime visibility (Vis), according to WMO and ICAO rules, can be estimated from the empirical and well qualified, Koschmieder law (at 550 nm), which connects the visibility (in km) with the atmospheric extinction coefficient $a_{aer}(\lambda,R)$ (in km^{-1}), as provided in Eqs. (10, 11).

It is well known that the human visual spectral range spans from 400 nm to 700 nm, peaking at 555 nm for daytime and 507 nm for night conditions, according to CIMO (Commission for Instruments and Methods of

Observation) for relative luminous efficiency of monochromatic radiation. By using the visibility versus the atmospheric extinction coefficient at 550 nm [10], we are able to have a good approximation of the above required values at daytime, at 355 nm.

In order to acquire the visibility values (Eqs. 10 and 11) NAVIS-T calculates the value of τ_{total} using Eqs. (13) and (20) (favorably using the trapezoid method) from the lidar's position to its pointing direction (typically 15^0 from horizontal). It checks at what range (R_1) of the lidar's position the $\tau_{total}(0,R_1) > 2*10^{-2}$, which according to METCON is the value of the extinction coefficient needed for the detection of cumulus cloud, with no visibility through it and corresponds to $\beta_{aer}(\lambda,R) \geq 2*10^{-3}$ m^{-1} sr^{-1}, with $C(\lambda,R) = 10$ sr^{-1} and $\alpha_{aer}(\lambda,R) > 2*10^{-2}$ m^{-1} (section 3).

Then, the NAVIS-T stops working at that range (R_1) and retains that range as the total visibility range at that time, according to WMO and ICAO rules for daytime visibility. As for the NAVIS-P application, the AOD starts to be measured from the maximum range (R_{max}) or from the range at which the lidar signal has useful information containing detection of the aerosols (R_2), towards the lidar's position.

From that automatic calculated or manually selected (cf. section 3) range (R_{max} or R_2 - user defined) and when $\tau_{total}(R_{max}, R_3) > 2*10^{-2}$ or $\tau_{total}(R_2, R_3) > 2*10^{-2}$ (for the reason mentioned before), the visibility is equal to that range (R_4) where:

$$R_{max} > R_2 \geq R_3 \quad \textbf{(15)}$$

and $R_4 = R_{max} - R_3$ or $R_4 = R_2 - R_3$ (user defined) **(16)**

counting from the range of R_{max} or R_2 (user defined). In both cases, if $\tau_{total}(0,R_{max}) \leq 2*10^{-2}$ through the whole distance (R_{max}), then the visibility is equal to R_{max}. The outcome for NAVIS-T and NAVIS-P accordingly, is that: "The visibility of tower controller is R_1 (or R_{max})" and "The visibility of the pilot from R_{max} (or R_2), is R_4 (or R_{max})".

3. METCON ALGORITHM

METCON (METeorological CONditions) algorithm is able to provide meteorological conditions like clouds, haze, fog, etc., versus distance (R), for any vertical or slant range lidar measurements. The same 3D scanning lidar and the above-mentioned techniques and data, can be used to characterize the atmospheric conditions (fog, haze, etc.), plus the visibility with NAVIS.

The METCON algorithm in our case is taking into account [10] and observes the different $C(\lambda,R)$ between different atmospheric conditions like Haze, Fog, Moderate fog, cloud etc. Afterwards according to values of $\beta_{aer}(\lambda,R)$ and $\alpha_{aer}(\lambda,R)$ taken from [9] concerning those atmospheric conditions. A combination between atmospheric conditions and the above mentioned values is being made and a visualization of the atmospheric layering of those conditions is produced (Figs 2a, 2b, 3a, 3d).

In Fig. 2 a case study of the application of NAVIS and METCON algorithms is shown, where the tower visibility from lidar's vertical pointing direction is found to be 1512 m and pilot's visibility is 1370 m from the range of 3000m. A lidar pointing to the vertical is been chosen because of the large data availability at LRSU-NTUA [11] at different times and different months along several years.

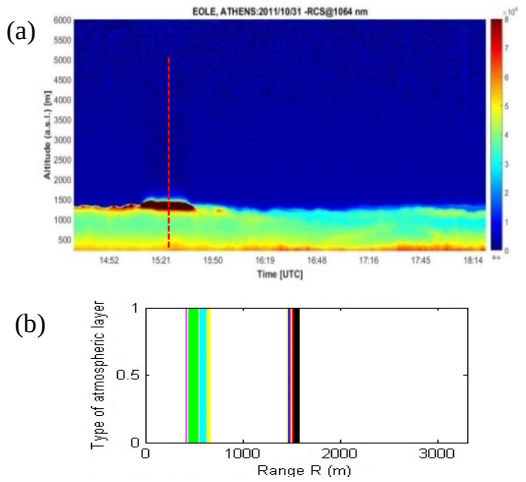

Fig. 2. a) RCS signal acquired at 1064 nm by the LRSU-NTUA (31-10-2011), b) NAVIS and METCON algorithms applied in 3D lidar data pointing to the vertical (355 nm), at 15:29:50 UTC, starting at 417.5 m above ground level up to 3000 m. Where Purple is "Thin Fog", Red is "Moderate Fog", Light Blue is "Light Haze", Green is "Haze" and Black is "Cumulus Cloud". Tower visibility is 1512 m and pilot's visibility is 1370 m from the range of 3000 m.

4. VASPAT-L/D ALGORITHM

In VASPAT–L/D we calculate $\beta_{aer}(\lambda,R)$ (and/or $\alpha_{aer}(\lambda,R)$, RCS) in the vertical or slant range (R) after range calibration of our lidar system for slant range measurements using the LADDER technique, calculation of RCS (cf. Eq. 5) and denoised the lidar signal. The entire process can be made upon all the received lidar data signals in a timeframe of an hour or less [12] (Eqs. 1-6). In this work, we chose to use settings appropriate for $\beta_{aer}(\lambda,R)$ (Eq. 3). However, the performing of the algorithms remains the same, with different setting values, for different kinds of measurement types, as analyzed below.

Next, the calculated values of $\beta_{aer}(\lambda,R)$ (Eq. 3) are being 'cut' into smaller 'space filters' in order to create different kind of 'mathematical tools' (conditions) for processing. In this work we have used 12 different 'space filters' (G1 to G269) from 7.5m (1 bin) to 2017.5m (269 bins),

$$G3 = 3*bin = 3*7.5(m) \quad \textbf{(9)}$$

(G3 represents the 'space filter' of the package of 3 bins).

Afterwards, we check if the calculated $\beta_{aer}(\lambda,R)$ values in any of these filters are greater than $8*10^{-7}m^{-1}sr^{-1}$ with $C(\lambda,R) = 50sr$ ($\alpha_{aer}(\lambda,R)>4*10^{-5}m^{-1}$), as a value greater than this, for $\beta_{aer}(\lambda,R)$, means that atmospheric phenomena like

haze, fog, etc., are present, at 355nm. Then, we check if the $\beta_{aer}(\lambda,R)$ values in any of these space filters from a package of bins to the next package of equal number of bins, are greater than 10% (percentage produced statistically in a great number of measurements), in order to find out if the difference between the $\beta_{aer}(\lambda,R)$ values, is within normal oscillation of the coefficient of the same layer or has to do with some important change that denotes different layering. At the next step, the algorithm calculates the 1st $(d\beta_{aer}(\lambda,R)_{G3}/dR)$ and 2nd order derivatives $(d^2\beta_{aer}(\lambda,R)_{G3}/dR^2)$ of all space filters, at any distance.

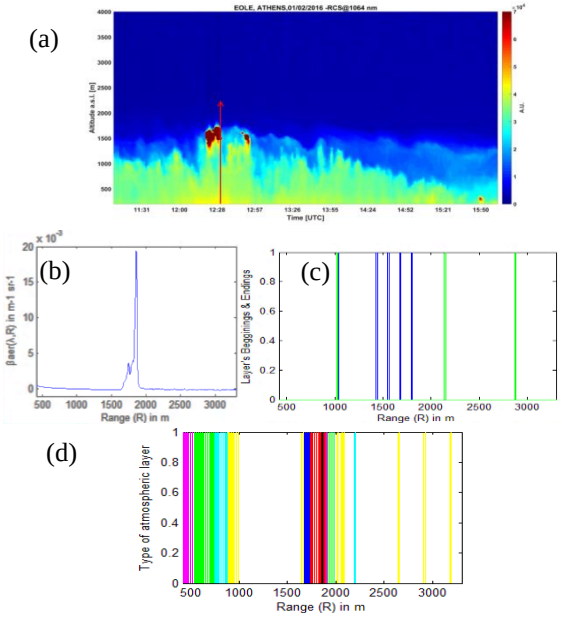

Fig. 3. (a) RCS signal acquired at 1064nm from LRSU NTUA data at 12:29:40 UTC of 01/02/2016 (b) Calculated $\beta_{aer}(\lambda,R)$ at the time of measurement (c) VASPAT–L/D algorithm in use at a 3D lidar in vertical position, at 355nm, starting at 417.5m above ground and more than 3000m ending. With blue color are the 'beginnings' of an atmospheric layer and with green color are the 'endings', in agreement with (b), (d) Colored visualization of meteorological conditions according to Fig. 1, starting at 417.5m above ground level up to 3000m with METCON algorithm outcomes.

Then, we check if these 1st order derivatives have the same sign (positive sign or negative one) for a number of continuing space filters like G2, G3 and G5. So, if the 1st order derivatives with the same sign correspond to values greater than 12o angle change (statistically produced for estimating serious change of layering, not a layering normal oscillation – user dependable), we store these values at distance (R_x). A 'beginning' of a layer produced by positive values of 1st order derivatives (>12o angle change of values of $\beta_{aer}(\lambda,R)$ - recommended) and positive values of 2nd order derivatives, plus 10% change of averaged $\beta_{aer}(\lambda,R)$ values, from the next package of equal number of bins. In accordance, an 'ending' of a layer produced by negative values of 1st order derivatives (>12o angle change of values of $\beta_{aer}(\lambda,R)$ - recommended) and negative values of second order derivatives, plus 10% change of averaged $\beta_{aer}(\lambda,R)$ values from the next package of equal number of bins. Above, in Fig. 2 (c), with blue color are the 'beginnings' and with green color are the 'endings' of a case presented for that purpose (where two or more continuing blue or green color lines, without any different color line in between, shows that $\beta_{aer}(\lambda,R)$ (and/or $\alpha_{aer}(\lambda,R)$, RCS) continues to go higher (blue line) or lower (green line) in quantity (value), probably in different kind of layer and in this way, we can have an easier perception of L and D).

Common layering altitudes - heights are being tracked among equal and different continuing space filters and an average is being produced for these altitudes, in terms of 10 to 15 range - height bins (75 to 107.5m spatial tolerance). In this way we are able to produce, in total, atmospheric layering (VASPAT–L) and we are able to have a clear understanding of the distribution (VASPAT–D) of $\beta_{aer}(\lambda,R)$ (and/or $\alpha_{aer}(\lambda,R)$, RCS) in a 3 dimensional way surrounds a 3D lidar system or an area, for example of an airport.

5. VASPAT-PBLH ALGORITHM

To begin with, we already have our lidar in, favorably, vertical position and it is recommended in less than 30o from vertical, for purposes of capability of the lidar system to reach molecular heights at the receiver. We continue measuring for at least 15 to 20' (user dependable), in vertical and acquire at least 15 or more lidar data files. It is time for the creation of the 'time filters' of the VASPAT algorithms.

These filters have to do with the 15 or more data files that we are keeping track from. In other words, we are keeping track of the layering and distribution at LAYER matrix filled with 'beginnings' and 'endings' from VASPAT-L/D but this time, we check only the produced 'endings'. In this algorithm we tread PBLH as a layer 'ending' with no 'beginning' in every specific small time frame of 15 or more minutes, for vertical pointing measurements. The ideal would be ~30' of recording time of $\beta_{aer}(\lambda,R)$, but in any case less than 60' [12] where PBLH could have a small or medium change especially in medium weather conditions. The idea is to take advantage of that unique characteristic of PBLH that looks like a common 'ending' in our time scaling VASPAT-L/D algorithm.

Then, we check the heights of those 'endings' and if they exceed a common PLBH area for that time of the year and for our location (colder or hotter climates with lower or higher commonly PBLHs, accordingly – user provided). We add (and subtract accordingly), some height from that area of commonly PBLHs (user adjustable) in order to produce a wider area of height search and in this way, we exclude larger height 'endings' in order to exclude the possibility of capturing higher cloud 'endings' rather than PBLH and we also exclude lower layer 'endings', mistaken as PBLH (user dependable). It is noted that the common PBLH provided by the user is not mandatory for the rest of VASPAT–PBLH algorithm to produce its result concerning PBLH.

Afterwards, we check which is the most common 'ending' layer in all times series of 15 to 20' (maximum 1h [12] of our 15 or more data files. This is done because we expect that the present PBLH will not vary much (more than 300 to 500m [12] in such a small time period. Even in a case of disturbed weather conditions, where a sharp change is occurred, it will have a scaling that will be easily observed and captured by our measuring track records of measurement, which have a time scale of a maximum around 1h. Then, an average height of that measurements of most common 'endings' in terms of 10 to 15 height bins difference (user adjustable) will be provided as PBLH, even if it is dynamically and violently changing. If there are more than a common 'ending' exists with the same higher frequency, several more files added to that search and more than 15 data files might needed to add to process, in order to have at least a two times more common 'ending' than the second most appeared one (recommended).

So, for disturbed weather conditions, 2 or maximum 3 previous PBLH retrievals might be of use (recommended), but in more soft weather conditions, 3 or even 4 PBLH retrievals and more, could be of valuable use. The reason is that in disturbed weather the PBLH might change dramatically each time and in easier layered weather conditions, more recording time might needed to spot clearly, the exact PBLH. The maximum recording time that we could take into account is recommended to be 1h or less.

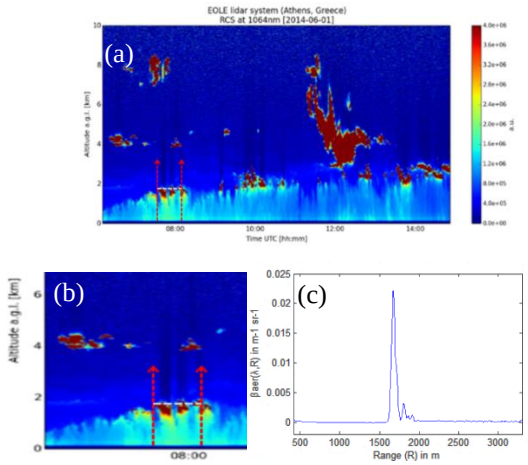

Fig. 4. (a) RCS signal acquired at 1064nm from LRSU NTUA data (1/6/2014) begins at 06:00 UTC. (b) Zoomed file of the previous figure for the time period of 07:44:30 till 08:07:50 UTC where VASPAT–PBLH provided PBLH estimation. (c) Indicative record of $\beta_{aer}(\lambda,R)$ at that period of time (07:46:10 UTC). The PBLH produced at 1872.5m is in total agreement with (c). The red arrows denote the recording timeframe and the white line denotes the averaged PBLH, as produced by VASPAT algorithms.

The algorithm can be restricted by a minimum and maximum altitude of commonly PBLH area, of 1000 to even 5000m, depending on the geographical position (latitude) of the measurement and the most common PBLH values through previous years, at the corresponding time the measurements were taking place. The exact PBLH value will be delivered, after an average of most probable common 'endings', with slightly different heights, that have left and have been chosen for the PPBLH matrix and then the most probable one will be given as PBLH (Fig. 4).

6. CONCLUSIONS

In this paper we presented several novel algorithms and technique applied in vertical and slant range lidar measurements to calculate horizontal, slant and vertical visibility for tower aircraft controllers, meteorologists, and for the pilot's point of view, as well as for the detection of atmospheric layering and distribution of $\alpha_{aer}(\lambda,R)$ and/or $\beta_{aer}(\lambda,R)$ in 3dimensions, along with the detection of the Planetary Boundary Layer Height. We also provided typical examples based on real lidar data obtained over Athens by the EOLE system. The present work was evaluated successfully through LRSU NTUA for the above required outcomes.

Funding Information. This research has been co-financed by the European Union and Greek national funds through the Operational Program Competitiveness, Entrepreneurship and Innovation, under the call "RESEARCH-CREATE-INNOVATE" (project code: T1EΔK-03147).

Co-financed by Greece and the European Union

References

1. W. Vieeze, J. Oblanas, R.T.H. Collis, "Slant range visibility measurement for aircraft landing operations" (SRI, February 1972).
2. R. H. Kohl, "Discussion of the interpretation problem encountered in single wavelength lidar transmissometers", J. Appl. Meteor. **17**, 1034 (1978).
3. V. A. Kovalev, W. E. Eichinger, "Elastic Lidar," Wiley Interscience (2004).
4. J. Klett, "Stable analytical inversion for processing lidar returns," Appl. Opt. **20**, 211 (1981).
5. J. Klett, "Lidar inversion with variable backscatter extinction ratios," Appl. Opt. **24**, 1638 (1985).
6. A. Ansmann et al "Combined Raman elastic-backscatter lidar for vertical profiling of moisture, aerosol extinction, backscatter, and lidar ratio," Appl. Phys. **B55**, 18 (1992).
7. E. Landulfo, A. Papayannis et al, "Tropospheric aerosol observations in São Paulo, Brazil using a compact lidar system", Int. J. Remote Sens. **26**, 2797 (2005).
8. G. Pappalardo et al, "Aerosol lidar intercomparison in the framework of the EARLINET project. 3. Raman lidar algorithm for aerosol extinction, backscatter, and lidar ratio", Appl. Opt. **43**, 5370 (2004).
9. W. L. Wright et al, "A preliminary study of air pollution measurement by active remote sensing techniques," NASA, CR-132724 **C89** (1966).
10. R. M. Measures, "Laser remote sensing. Fundamentals and Applications," Krieger, Sys No 9247, MEA 621.3678 (1992).
11. http://www.physics.ntua.gr/~papayannis/
12. R. B. Stull, "An Introduction to Boundary Layer Meteorology", Kluwer Academic Publishers, Dordrecht (2013).